JMEPEG (2004) 13:517-529
DOI: 10.1361/10599490420665

1059-9495/$19.00

Testing of General and Localized Corrosion of Magnesium Alloys: A Critical Review

Edward Ghali, Wolfgang Dietzel, and Karl-Ulrich Kainer

(Submitted June 4, 2003; in revised form April 20, 2004)

The degradation of materials generally occurs via corrosion, fatigue, and wear. Once a magnesium (Mg) alloy is chosen for a certain application, corrosion testing is generally required as a function of the expected service environment, the type of corrosion expected in service, and the type of surface protection, depending on the material and its use in the intended surface. In the absence of appropriate standards for the testing of magnesium alloys, a brief summary of the various procedures of accelerated electrochemical and corrosion testing of Mg alloys that have been adopted by different schools is given, accompanied by some critical comments for future work. Hydroxide, hydroxide-chloride, and corrosive water formulated according to American Society for Testing Materials (ASTM) standard 1384-96 are considered to evaluate general corrosion, localized corrosion, and corrosion influenced by metallurgical parameters. The influence of agitation, oxygenation, pH, and temperature are discussed. Surface cleaning, superficial microstructure, and surface preparation for testing are discussed. Appropriate electrochemical methods that can be applied to this relatively new and electrochemically active structural material are described. Corrosion potential measurements, polarization, impedance, noise electrochemistry, and surface reference electrode technique are recommended as valuable methods for evaluating the resistance of existing or experimental alloys to these types of corrosion. Corrosion kinetics and varying properties of the solution at the alloy/solution interface are examined. A critical description of the relevance and importance of these methods to corrosion testing of Mg alloys is given.

Keywords corrosion testing, electrochemical corrosion measurements, general corrosion, localized corrosion, magnesium alloys

1. Prior Considerations to Mg Testing

One of the most important and indispensable steps to promote the use of magnesium (Mg) as a structural material is the development of standardized testing procedures that can be accepted by the interested organizations and customers, as well as by the government agencies that regulate them. Precise testing standards can give the manufacturer and the user a solid and safe basis for the fabrication, use, and performance of Mg alloys. Corrosion testing can also help in the development of both new alloys with better corrosion performance and efficient coatings. Properly conducted corrosion testing can mean the saving of millions of dollars and, more importantly, can save lives by preventing premature failures of structural components. Determining the best material to meet a requirement and predicting the probable service life of a product or a structure depends enormously on environmental conditions and on variations of the metal/liquid interface properties as a function of time. The selection of the appropriate Mg alloy for the targeted environment should help to establish Mg alloys as light structural materials for this century. Testing can help in selecting and/or developing suitable inhibitors and/or efficient coatings.[1]

The degradation of materials generally occurs via three well-known mechanisms, which are frequently interconnected (i.e., corrosion, fatigue, and wear). In selecting corrosion tests, generally, four factors should be studied and adapted to Mg and Mg alloys. These are 1) the expected service environment, 2) the type of corrosion expected in service, 3) the primary material requirements of the application, which should not be excessively degraded by corrosion, and 4) whether the material requires surface protection for use in the intended environment.[2] The most reliable prediction of performance is service experience, followed closely by field testing, because both are based on the actual environment. Previous performance data for the alloys of interest, or one as close to a certain environment as possible, should be examined before planning laboratory tests. For example, references concerning corrosion data, such as those of NACE,[3] ASM,[4] De Renzo,[5] and Schweitzer,[6] should be considered. When service history is lacking, or when budget constraints prohibit field testing, laboratory corrosion tests are important for quality control, materials selection, and materials development. However, laboratory testing can be misleading if appropriate media and accelerating corrosive conditions are not closely related or do not simulate the service conditions.

Some form of surface protection is necessary for most of Mg alloys in outside structures. For the evaluation of protective coatings, considerations of the grain structure of the metal may not be relevant. However, the testing of coated Mg alloys should have some specific considerations pertaining to the quality of the coating, the interface, and the coated surface.

Edward Ghali, Department of Mining, Metallurgical and Materials Engineering, Laval University, Quebec, Canada G1K 7P4; **Wolfgang Dietzel,** and **Karl-Ulrich Kainer,** GKSS Research Center, Forschungszentrum GmbH, Institute for Materials Research, Center for Magnesium Technology, Geesthacht, Germany. Contact e-mail: edward.ghali@gmn.ulaval.ca.

This article is devoted more specifically to evaluating the noncoated surface of Mg and its alloys by some conventional and electrochemical methods. Methods are described that can be extrapolated to a bare surface of an electrochemically inert coating, assuming that the coating does not create special corrosion phenomena, such as a differential oxygen cell or a crevice.

1.1 Metallurgical Description and Sampling

A fabrication history describing the major steps together with an accurate analysis of the metal composition is necessary to characterize the material. Metallographic examination may also be necessary for the interpretation of corrosion test results, especially for new alloys or new production and/or processing routes. Cast or wrought alloys should be tested in the same surface conditions as those in which they are used. For example, the skin of some cast alloys can have a finer structure than the interior due to ingot cooling speed and has shown better corrosion resistance if used in the as-received or as-fabricated condition.[7]

1.2 Accelerated Electrochemical and Conventional Testing

For electrochemical corrosion, the properties of the medium at the interface should be considered in accelerated tests. Tests of the bare, unprotected metal are useful to establish a minimum required basis of performance, while the prediction of service life requires an evaluation of the coatings and a selection of maintenance procedures.[2] Corrosion rates tend to decrease as the electrolyte becomes spent and saturated with Mg ions, while contamination of a pure solution can increase or decrease the corrosion rate, depending on the quantity of magnesium hydroxide. Consequently, flow rates and the ratio of the area of metal surface to the volume of the solution should be considered. It is recommended that electrochemical testing should be generally accompanied and interpreted by natural and accelerated corrosion tests.

The number of replicates can be deduced by considering the objectives of the test, the accuracy and precision required for the test, the known reproducibility of the test, and the cost of doing the test. The American Society for Testing and Materials (ASTM) recently made it mandatory that statements on the precision (reproducibility) and bias (systematic error) of a material be included in every standard. For example, pitting can depend on intrinsic properties of the metal, which can be irregularly distributed and may depend on the hazardous nucleation of a pit, and so a statistical approach is highly recommended if duplicates or triplicates are not available.[8]

2. Designation, Uses, and Properties of Mg Alloys

2.1 Designation of Commercial Alloys

Commercial Mg casting alloys are identified by a standard ASTM/SAE system for alloy and heat treatment designation[9]:

1. Two capital letters indicate the two principal alloying elements in order of decreasing percentage. The letters are: A, aluminum; E, rare earth; H, thorium; K, zirconium; M, manganese; Q, silver; S, silicon; Z, zinc, and less frequent metals such as, for instance, W for yttrium.
2. Two digits indicate the nominal percentage of the two principal elements in the same order as the letters.
3. A capital letter distinguishes between alloys of the same major composition that differ in minor elements. The letter represents a chronological sequence of development.
4. A letter and number indicate the condition or temper, such as

- F, as-cast,
- T4, solution heat treated,
- T5, artificially aged only,
- T6, T61, solution heat treated and artificially aged, and
- T7, solution heat treated and overaged.

2.2 Uses and Properties

The use of Mg as a structural material is a major factor in the implementation of lightweight construction approaches in automotive engineering. One of the reasons for this is the commitment of the automobile industry to achieve a 25% reduction in average fuel consumption for all new cars by the year 2005 compared with 1990 levels. Apart from air resistance, the performance of a vehicle and fuel consumption are affected by rolling resistance and acceleration, both of which are dependent on mass.[10] Wrought products such as extrusions, forgings, sheet, and plate are also being used in a variety of different applications. There is a growing interest in the automotive industry in the use of wrought alloys. Aghion and Bronfin[11] stated that currently only 5000 tons of wrought Mg alloys are used per annum, compared with more than 125,000 tons of cast Mg. Thus, the situation in the automotive industry with respect to the use of Mg is completely different from that in the steel and aluminum industries, where most of the products are made of wrought alloys.

Mg has made significant gains worldwide in vehicle interior applications, replacing mostly steel stampings in instrumental panels, steering wheels, and steering column components. The overall demand for Mg alloys, other than for die casting, is expected to show only very modest growth, if any, over the next several years. However, high-pressure die casting continues to remain a promising long-term potential growth area. Special zirconium-containing casting alloys with rare earth elements, yttrium, silver, and zinc are used for parts operating at temperatures between 250 and 300 °C for extended periods of time. Sand-cast aerospace applications should also be mentioned.[9] It is widely accepted that the commercial Mg alloys AZ91D, AM60B, and AM50A offer a good balance between mechanical and physical properties at ambient temperature, excellent die castability, good corrosion resistance, ease of handling, and relatively low cost. An important material-intensive area exists in which improved elevated-temperature performance is required for products, such as drive-train components (e.g., gearbox housings, intake manifolds, oil pans, transfer cases, crankcases, and oil pump housings) for automobile applications.[12]

One potential exception in Mg processing is thixomolding, which is attracting considerable interest as an alternative for

replacing plastic injection moldings that are used in transportation applications and portable devices with Mg.[13] For example, the Mg content per vehicle is expected to rise from the present 3-4 kg to about 6 kg in 2005. Yet, this lags behind the use of aluminum, 123 kg of which are used per General Motors (GM) vehicle, for example.[14]

Recent growth has been stimulated by the AM series of Mg alloys. These alloys comprise excellent energy absorbing properties, enabling their use in safety-related applications such as steering wheels, instrument panels and beams, seats and structures, brackets, and inner door panels. Mg alloys, which are one-third lighter than an equal volume of aluminum alloys, offer many possibilities for the weight reduction of major heavy components such as engine blocks, wheels, gear-box casings, and front cradles.[11] In the power train area, GM and Ford lead the push for applications of Mg in four-wheel-drive transfer cases in high-volume truck production, while Volkswagen is aggressively expanding the use of Mg in manual transmission cases produced in both Europe and China. Only a limited number of body and chassis components are currently made of Mg. Mg applications with the highest growth potential are in instrument panels and steering structures.[14] As material for passenger seats, Mg was preferred over plastic, steel sheet, and aluminum gravity-casting designs. Mg die castings made of the high-ductile alloys AM50 and AM20 offered the best combination of high strength, extreme rigidity, low weight, and cost.[12] However, for automatic transmissions and engine applications (i.e., blocks and crank cases) in which the operating temperatures are significantly higher, new Mg alloys with better creep resistance have to be developed. The development of low-cost, corrosion-resistant coatings, and new Mg alloys with improved fatigue and impact strength will also accelerate the acceptance of Mg for chassis applications.[14]

Thixocasting is a well-established process for the semisolid forming of aluminum alloys, while thixomolding was especially developed for Mg alloys in an attempt to adopt machinery ideas from plastic molding.[15] Numerous applications for Mg housings produced by thixomolding can be found in the audio and electronic/information industries. The components are generally thin-walled and relatively small in size and are most commonly found in laptop computers, as well as in handheld devices such as cell phones and various types of cameras. With thinner cast sections, the solidification of the Mg melt would be accelerated to create a fine-grain microstructure. This is beneficial for corrosion resistance.[16] Most of these parts require a high-quality surface finish and are usually painted. Mg holds a unique combination of advantages over plastic in that it is 100% recyclable, has good heat dissipation, electromagnetic and radio frequency (RF) shielding, and it is light, rigid, and compact.[13] More than 40 different parts were thixomolded in 1997 with an overall production volume of 10 million pieces.[17]

Mg wrought alloys offer crucial advantages, such as superior mechanical properties. Unlike casting components, they are weldable and offer the possibility of thermal treatment and an improved ductility and are therefore interesting for a wide range of applications.[18] It is conceivable to use them in various areas, depending on the loads exerted on the component in applications such as outer body panel structures, window frames, seat structures, and carrier or support structures. Structures made of Mg extrusions are interesting for use in "bodies-in-white." However, forming behavior, corrosion resistance, and alloy development are areas in which further research is still required before Mg extrusions can be used in vehicles. Sheet forming with heated tools offers an interesting method for the production of large-area and very thin-walled, lightweight components made of Mg sheets.[19] The further application of Mg wrought products will mainly depend on the progress made in surface treatment, joining techniques, and cost-reduction programs.[10]

3. Testing Solutions for General Corrosion, Passivation, and Localized Corrosion

Most Mg-testing solutions include chloride or sulfate ions in neutral or alkaline media and are used to evaluate general and localized corrosion. Buffer solutions and saturation of the solution with magnesium hydroxide, as well as surface cleaning, have been adopted by some schools.

3.1 Hydroxide Solutions

With pH increasing above 10.2, the point at which magnesium hydroxide is formed, the effect of impurities both in the metal and in the solution media is apparently overshadowed by the high tendency of film formation. When the pH exceeds 10.5, a value that corresponds to the pH of saturated magnesium hydroxide, a magnesium hydroxide film is formed on the surface, and Mg becomes very resistant to corrosion in alkaline solutions.[20] In deaerated 0.1 *N* sodium hydroxide solution (pH 13), even without sodium chloride additions, the corrosion potential (E_{corr}) of a Mg FSI alloy (e.g., Al 3.1% and Zn 1.3%) oscillated from passive to active values periodically. The addition of a strong oxidizing agent such as hydrogen peroxide (10 mL) maintained the potential in the passive region.[21] In NaOH solutions adjusted to pH 12, the protective properties of the passive layer were shown to be much better than that of the basic metal. However, the properties of the formed passive layer are generally a function of the base metal (less or more porous), containing some compounds of alloying elements. In a 1 *M* NaOH solution (pH 14), i.e., at a pH far above that of a saturated magnesium hydroxide solution, Mg should show a good active-passive behavior.

A 10% caustic solution is frequently used for cleaning Mg at temperatures up to the boiling point before testing and in practice. A deliberate increase of pH to about 10.5 by the addition of CaO or NaOH suppresses corrosion in a large volume of water. The beneficial effects of a calcium oxide treatment are the possible precipitation of undesirable metals such as copper in addition to the formation of a protective hydroxide. It has been observed that once attack is inhibited, and if it is uniformly distributed, an increase of the critical pitting potential and a delay in the onset of pitting usually occurs.[20] Soak cleaners are used as alkaline cleaning in concentrations of 30-75 g/L (4-10 oz/gal) and at 71-100 °C.[22]

3.2 Chloride, Sulfate, and Hydroxide Solutions

A sodium chloride solution (3%) has been used by Hanawalt et al.[23] to generate important data on the tolerance

limits and the individual or combined effects of impurities in Mg alloys. A 1 *N* NaCl solution with a normal pH of around 7 is recommended and has been used by some authors and compared with a 1 *N* NaCl solution adjusted to pH 11 by NaOH to show the influence of pH, and the passivation aptitude and passivation quality of the corrosion products formed. A solution of 5% NaCl saturated with $Mg(OH)_2$ at pH 9 can distinguish between the behavior of different Mg samples and is frequently used but not standardized. This can be accompanied by experiments in a 5% NaCl solution to show the influence of saturation with magnesium hydroxide.

Polarization curves obtained in a 1 *N* NaCl solution adjusted to pH 11 by NaOH showed different pitting potentials as a function of the microstructure.[7,20,23-26] A 2 *N* NaCl solution alone has also been used, but it seems to be aggressive, especially if Mg composites are tested.

Solutions of 0.1 *M* NaOH with additions of 0.005, 0.01, 0.02, and 0.03 *M* NaCl are used for the determination of pitting or filiform corrosion during a 24 h immersion period. Passivation and reproducible results are obtained by using an addition of 10 mL hydrogen peroxide (30%) in corrosion-pitting studies, preferably with pH adjustment to 11.[21] A 1 *N* sodium hydroxide solution saturated with Mg_2SO_4 can show the influence of the aggressive sulfate ion with reference to industrial media.[24-26]

3.3 Buffer Solutions

Buffered solutions generally do not correspond to the practical aspects of Mg corrosion, except for those buffered with high magnesium hydroxide concentrations, since this can simulate the interfacial corrosion of some Mg alloys in a non-stirred solution. In effect, in solutions with low concentrations and initial pH values of 7, 9, and 11, the pH value had changed to a value of approximately 10.5.[21] Borated boric acid buffer (pH 8.4) containing 0.001 *N* NaCl is advantageous for materials that are susceptible to pitting. The low percentage of sodium chloride and sodium hydroxide can give a controlled attack and reproducible results. Higher quantities of NaCl can also give reproducible results for situations that are less sensitive to agitation.[27]

A 0.1 *N* sodium borate solution (buffer pH 9.3) saturated with $Mg(OH)_2$ at pH 10.5 was used to measure corrosion rates at different strain percentages by the linear polarization method. It has been found that the borate anion acts as a corrosion inhibitor.[28] For strained specimens, an aerated sodium tetraborate (0.05 *M*) with a pH of 9.7 has been chosen by Bonora et al.[29] since the Mg surface can be covered by a protective layer and the pH is stable. It has been shown by Inoue et al.[30] that corrosion rates of cast pure or highly pure Mg AZ31 and AZ91 in deaerated solutions containing 10 g/L NaCl at pH 6.5 and a pH 9 borate buffer, depended solely on the pH of the solution. The corrosion rates were determined gravimetrically. This electrochemical behavior corresponds to the resistivity of the passive layer to anodic reactions. AZ91E was an exception. Higher buffer capacity masked the detrimental effect of the cathodic impurities by reducing the difference between local pH at cathodic and anodic sites. However, Gutman et al.[28] showed that the highest sensitivity to creep in the corrosive environment is observed in the alloy with the highest Al content in the AZ91D and AM50 Mg alloys tested in a 0.1 *N* sodium borate aqueous buffer solution at pH 9.3 or in the same solution saturated with magnesium hydroxide at pH 10.5.

3.4 The ASTM Standard D 1384-01 Corrosive Water

Corrosive water, formulated according to ASTM standard D 1384-96, has been used, either alone or saturated with magnesium hydroxide, to simulate the Mg alloy/solution interface that may contain important concentrations of magnesium hydroxide in stagnant solutions.[31,32] The ASTM corrosive water has been designed to distinguish between coolants that are definitely deleterious from the corrosion point of view. The corrosive water should contain 100 parts per million (ppm) each of sulfate, chloride, and bicarbonate ions that are introduced as sodium salts and is prepared using the anhydrous form of 148 mg sodium sulfate, 165 mg sodium chloride, and 138 mg sodium bicarbonate. Although the recommended temperature of the test for engine coolants is 88 ± 2 °C and the aeration rate is 100 ± 10 mL/min, Mathieu et al.[31] worked at room temperature (RT), and the solution was exposed to atmospheric oxygen and was not agitated. It has been shown that the ASTM corrosive water alone, or saturated with magnesium hydroxide, is appropriate to distinguish between the electrochemical corrosion resistance of high-pressure, die-cast and semisolid cast AZ91D Mg alloys. Also, Adeva-Ramos et al.[32] examined pitting corrosion by immersing samples in the ASTM standard D 1384-01 corrosive water at pH 8.2. This was followed by potentiodynamic polarization for the determination of pitting potential in the same solution but saturated with $Mg(OH)_2$ at pH 10.6. The first solution can be considered as moderately aggressive, while the second solution simulates the metal/solution interface and can give lower corrosion rates.

4. Open Circuit E_{corr} Measurements

To get a stable potential, a time interval between 20 and 60 min has been considered by several authors.[29,31,33,34] However, for some alloys in certain media, a relatively varying potential can be obtained even after 1 h. The potential of the α-phase Mg_4Al is −1.82 V_{SCE} (−1.58 V_{SHE}), and that of the β-phase $Mg_{17}Al_{11}Zn_1$ is −1.23 V_{ECS} (−0.99 V_{SHE}) in ASTM D 1384 water at pH 8.2 and RT. The aluminum concentration in the primary α-phase is 3 wt.%, whereas it is only 1.8 wt.% in a die-cast alloy. Lunder et al.[35] and Beldjoudi et al.[36] showed a decrease of both the corrosion current density (i_{corr}) and the E_{corr} with the increase in Al content in a solution of 5% NaCl saturated with $Mg(OH)_2$. In a deaerated solution, Baril and Pebere[37] stated that as the concentration of sodium sulfate decreases from 0.1-0.01 *M* Na_2SO_4, the E_{corr} shifts toward more noble (positive) potentials of about 100 mV. The current densities were ≥10 mA/cm^2 for 0.1 *M* Na_2SO_4 and were halved for 0.01 *M* aerated solutions. In deaerated solutions, the E_{corr} of pure Mg is more noble (positive) and the anodic current densities are lower, when compared with that of the aerated solutions. This was attributed to the absence of bicarbonate ions and carbon dioxide gas, which is present in the natural environment.[37] An oxidant such as chromate shifts the poten-

tial in the more anodic direction (i.e., a more noble value) and reduces the i_{corr}.

5. Some Conventional Testing Methods

5.1 The Weight-Loss Method, and the Salt-Spray Test and Cyclic Tests

5.1.1 The Weight-Loss Method. The weight loss of a specimen was measured by dissolving the corrosion products in a hot chromic solution. The specimen was washed with distilled water and dried quickly in hot, flowing air. Then it was put into a 100 g/L CrO_3 solution at about 90-95 °C for about 5-10 min. After that, the specimen was washed with distilled water, dried, and weighed.[38] Gravimetric studies have been used by several investigators. This approach can be accompanied by some other methods such as atomic absorption, and spectrophotometric and calorimetric methods to determine the levels of Mg and alloying elements in the solution. The use of highly pure analytical quality reagents is recommended, and the magnesium hydroxide reagent can be avoided, preferably as an electrolyte.

To reduce the error caused by the dissolution of the uncorroded areas and substrate under the corrosion products during removal of the corrosion products, an uncorroded specimen is usually used as a reference in the chromic cleaning process.[38] Weight loss increased with increased chloride concentration.[21] The weight-loss method is not capable of measuring corrosion rates over short periods of time since in salt water, for example, as the corrosion reaction proceeds, the pH of the solution increases, and $Mg(OH)_2$ precipitates on the surface of the sample often cause a weight gain.[39]

Hanawalt et al.[23] have used weight-loss measurements taken from samples that were 25.4 × 38.1 mm with a thickness of 6.35 mm. Complete removal of the corrosion products was performed by a 1 min immersion in a boiling 20% CrO_3 solution containing 1% silver nitrate.[23] The usual boiling 20% $H_2Cr_2O_4$ solution in water is used to remove corrosion products from Mg and Mg alloys without attacking the base metal, while the silver nitrate is expected to form a fine precipitate of Ag_2CrO_4 that can react in turn to precipitate chloride ions that can be carried away from the corrosion products.[40] Molded samples are preferred to control the conditioning of the surface, and for potential recording for the first hour and at the end, however, a big surface in this case is not practical. Triplicates are recommended. Hanawalt et al.[23] have successfully compared some selected Mg alloys to pure Mg (e.g., WE43, which has good mechanical properties and is widely used). AZ91E has the lowest corrosion rate for Mg alloys, and AZ91D has good mechanical properties and low impurity levels and behaves in a way that is acceptable for many applications in certain corrosive media.[23]

The salt-spray test according to ASTM standard B 117-01 was carried out for 360 ks (100 h) using a solution of 0.86 mol/L NaCl. A corrosion rate of 0.018 mg/cm^2/d was obtained for an AZ91D alloy that had been prepared by thixomolding with an 0.8 mm thickness. This rate is almost 40% of that of the conventional cast alloy.[14] The samples (rods 40 mm in diameter and 10 mm in thickness) are exposed for 7 days to ASTM standard D 1384-87 corrosive water (pH 8.2) without and saturated with magnesium hydroxide at pH 10.6, and are maintained at RT, without stirring, to yield a solution volume five times that of every exposed square centimeter.[31]

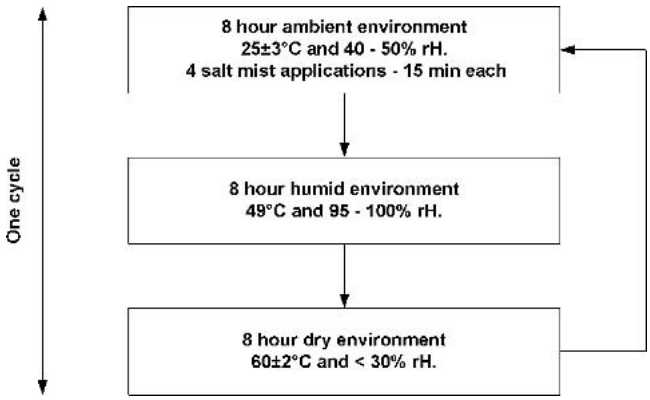

Fig. 1 GM adopted cyclic testing GM9540P. One cycle represents 1 day of exposure (Skar and Albright[41]).

5.1.2 The Salt-Spray Corrosion Test. The salt-spray corrosion test normally used to determine corrosion behavior is based on measuring the weight difference of the samples before and after the tests.[7] It is slow (3-10 days) and labor intensive, and it is error prone due to the cleaning procedure used. The corrosion samples also lose weight due to crumbling during the tests.[39] The salt-spray method determines the overall corrosion rate, which also includes weight loss due to disintegration, and this could result in misleading data depending not only on corrosion rate but also on the aptitude of the alloys to disintegrate.[39] Salt spray with a highly conductive electrolyte and continuous wetting of the sample surface is very aggressive for galvanic corrosion and consequently also for the corrosion testing of Mg. The corrosion mechanism of Mg alloys is attributed to microgalvanic corrosion between the matrix, and the noble intermetallic particles and secondary phases. This corrosion is strongly promoted in salt spray due to the presence of a very conductive electrolyte and the continuous wetting of the surface. Despite the poor correlation to real-life applications, salt-spray testing is commonly used to investigate the corrosion performance of die-cast Mg.[41]

5.1.3 Cyclic Corrosion Tests. For alternate immersion-emersion, Hanawalt et al.[23] carried out experiments in 3% NaCl solution for 16 weeks. The cycles consisted of 30 s in the solution followed by 2 min in air. During the latter time period, the specimens did not completely dry. The cyclic corrosion test currently used is that of GM9540P (Fig. 1).

Unfortunately, there is limited published experience about the correlation between the GM test and the life of automotive components that are made of Mg. It is, however, accepted that cyclic corrosion testing gives far better correlation to service than does salt spray. For zinc-plated and coated steel, GM9540P-cycle B (16 cycles in duration) was one of the tests showing the best correlation to an on-vehicle exposure test. The cyclic corrosion test uses a less conductive electrolyte and combines drying/wetting of the surface; it is thus less aggressive. For some applications, this test may be too mild due to the short time of the salt mist application and the lack of deposits of mud and dirt with hygroscopic salts.[41]

5.2 Amount of Hydrogen Gas Evolved and pH Measurements

5.2.1 Volume Measurement of Evolved Hydrogen. The overall corrosion reaction of Mg in aqueous solutions at its E_{corr} can be expressed as follows:

$$Mg + 2H_2O = Mg^{2+} + 2OH + H_2$$

The evolution of 1 mol of hydrogen gas corresponds to the dissolution of 1 mol of Mg. The contribution of oxygen reduction to the cathodic process is neglected. It is believed that, particularly in aggressive solutions such as NaCl, the cathodic reaction is mainly hydrogen evolution and the contribution of oxygen reduction is practically negligible.[38] The experimental setup can be designed in such a way that hydrogen evolution from the undermined particles can also be collected together with the hydrogen from the Mg specimen.[38] The dissolution of some alloying elements can cause error since the corrosion rate is based on the Mg dissolution reaction. Some alloying elements, however, can also produce hydrogen, which to some extent reduces the error. This method can reveal the instantaneous corrosion rate, and the changing corrosion behavior of Mg and its alloys.

The accuracy of this method could be affected by some corrosion products that are stuck on the specimen surface, so it is best used for short-term immersion experiments. It is difficult to determine whether the hydrogen evolution rate is more accurate than the weight-loss measurement. However, compared with the estimation of corrosion rates based on polarization curves, hydrogen evolution collection is undoubtedly very reliable.[38]

5.2.2 Evolution of pH Measurements. The principle of the method is based on measuring specific ions (such as hydrogen (H) cation or Mg cation) by an ion-selective electrode in a corrosive environment such as 5 wt.% NaCl solution in distilled water. The variation of ion concentration with time is recorded, and the corrosion rate is calculated. Weiss et al.[42] gave the following experimental details: The sample size was 40 × 30 × 15 mm, and it was machined, thoroughly washed with acetone, and dried in air. A solution was made of 5 wt.% NaCl in distilled water, for example. The solution volume was 1 L and was boiled for CO_2 degassing and kept under argon bubbling for the entire test. Figure 2 gives a schematic presentation of the evolution of pH as a function of time for Mg and some commercial alloys.

The corrosion rates of each sample were calculated from several measurements (pH between 10 and 15), which were taken at an interval of 1 min and showed good agreement with those obtained by weight-loss methods.[42] As in the volumetric method of H determination, the oxygen catalysis of the cathodic reaction, the dissolution of oxides or alloying elements can cause some error in the calculation of the corrosion rate.

5.2.3 Controlled pH Measurements. In the last two methods, the H concentration of the salt solution decreases significantly with time, causing the precipitation of $Mg(OH)_2$ on the surface of the samples. This affects the intrinsic corrosion rate. This technique was used to compare the corrosion behavior of newly developed creep-resistant Mg-Al-Ca (AC) alloys with several known Mg alloys. Tiwari and Bommarito[39] recently succeeded in determining the intrinsic corrosion rate of these alloys and thus in evaluating the performance of new or experimental alloys. The method measures the dissolution rate of Mg alloy samples in a 5% NaCl solution under a controlled pH. It is fast (<5 h) and is capable of discerning the effect of small compositional changes or different tempers on the corrosion behavior of selected Mg alloys. As a Mg alloy sample dissolves in a 5% NaCl solution, the dissolution rate is determined by measuring the amount of HCl added to the NaCl solution to obtain a controlled pH of between 5 and 7. The corrosion curve showing the amount of HCl added (in milliliters) as a function of time generally has three portions (Fig. 3). The first portion corresponds to the reaction of magnesium oxide with H ions, producing water and Mg ions. The corrosion rate can be constant from the beginning if an excessive oxide layer on the surface is not present and this portion is not observed.

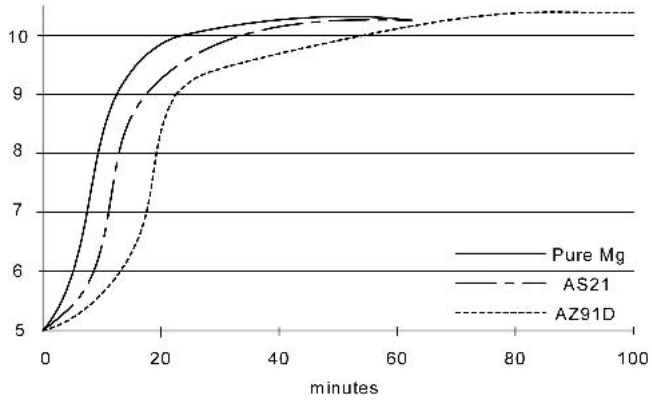

Fig. 2 A schematic presentation of pH evolution as a function of time for Mg and two commercial alloys in a 5% NaCl solution (Weiss et al.[42])

In the middle or second portion of the corrosion curve, the rate is exclusively controlled by the reaction $Mg + 2H^+ = Mg^{2+} + H_2$. The corrosion rate is determined from the slope of the curve where the dissolution rate reaches a steady state. This represents the intrinsic corrosion rate of the alloy. In the third portion of the corrosion curve, a disintegration of Mg caused by the H_2 bubbles in form of fine particles was observed that increases the effective surface area and thus the corrosion rate. The rate of corrosion seems to be closer in the second and third portions of the curve; however, this can depend on the microstructure and the composition of the alloy.[39]

This method is capable of discerning the effect of small changes in alloy composition on corrosion rates. An addition of small amounts of Si (0.3%) to AC alloys increases the corrosion rate, while Sr (0.07%) reduces it. It was also shown that the corrosion rate of AC52 (Mg-5%Al-2%Ca) is comparable to AZ91, meeting one of the several design criteria for new, creep-resistant alloys.[39]

5.3 Potentiodynamic Measurements

The polarization curve may exhibit Tafel linear regions; however, the corrosion current cannot be extrapolated from this linear region. The reason for this is that the reaction

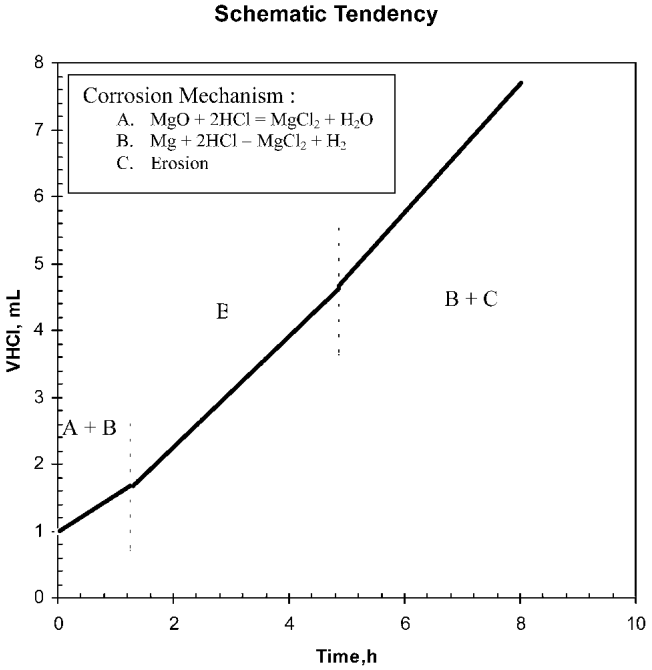

Fig. 3 A schematic presentation of the three regions of attack of a commercial alloy, AC53, in a controlled pH between 5 and 7 using 1 *M* HCl (Tiwari and Bommarito[39])

mechanism around the E_{corr} is different from that in the Tafel region, due to the negative difference effect. This is a special electrochemical phenomenon of Mg and its alloys, in which the H evolution rate increases during anodic polarization. It is also possible that much of the negative difference can be due to the disintegration of the metal into fine particles, which has been described as the chunk effect.[43] Hence, the determination of a polarization curve is not a reliable method for estimating the corrosion rate of Mg and its alloys.[38] Another method to assess the corrosion resistance of Mg alloys is linear polarization, which is based on the polarization resistance over the range of the $E_{corr} \pm 10$ mV (5-20 mV is acceptable) and on the coefficients of the Tafel slope.[8,44-46] However, due to passivation or the negative difference effect, the anodic Tafel slopes are not easily determined so as to give more precise values of the corrosion current by the linear method.

5.4 Corrosion Current Measurements

The working electrode generally consists of a cylindrical rod, on the order of 1 cm^2 in size, that gives a good representation for Mg alloys. It is more advisable to have a round surface to avoid the phenomenon of corrosion around the edges (concentration of corrosion current and products). The solution volume can be on the order of 100 mL/cm^2 of the metal surface. It is recommended that there be a rather stable open circuit potential (E_{oc}) before scanning. The potentiodynamic scan can start at −250 mV versus the E_{corr} to an anodic potential, at which point the current density should not exceed 1 mA/cm^2. The potential scan rate can be on the order of 0.1-0.2 mV/s however; depending on the composition, the microstructure of the examined alloy, and solution characteristics, slower scan rates could be advantageous. Due to the possible formation of magnesium hydride compounds, which can change the properties of the natural corroded surfaces, cathodic cleaning of the surface at moderate or high cathodic potentials, as well as very slow stationary potential scanning, is to be avoided. It has been found that the level of cathodic polarization, adopted normally to clean the metallic surface of oxide films, can influence the form and characteristics of the polarization curves.[21] However, higher cathodic potentials have been used, even a polarization of −4 V. No reliable data can show at what potentials magnesium hydrides may form and thus change the electrochemical properties of the Mg surface. It is preferred to start with two identical surfaces of the same sample and scan one to generate the cathodic curve and the other to generate the anodic curve in starting from the steady E_{corr}.

The polarization resistance method has been used successfully for comparison purposes to determine i_{corr} as a function of the elongation for AM50 and AZ91D commercial alloys. In an aerated borate solution at pH 9.7 and RT, the corrosion rate passes over a maximum in relation to the increase in plastic deformation. Also, the most negative value of the E_{oc} corresponds to the maximum value of the corrosion rate.[29,31,47] The electrochemical impedance spectroscopy at open circuit or at imposed potentials gives polarization resistance (R_p) values in considering the solution resistance. The $1/R_p$ corrosion current calculations for AM50 and AZ91D alloys were found to give a parallel classification to those obtained from potentiodynamic measurements using the linear polarization method (0.2 mV/s) in aerated buffer solution at pH 9.7.[29]

6. Electrochemical Evaluation of Subtypes of Localized Corrosion

Every subtype of localized corrosion may have its appropriate methods for assessing corrosion rates besides the use of general corrosion rate measurements such as weight loss. For example, pitting requires micrometer gauges and statistical considerations, while intergranular attack necessitates metallographic examination.[1]

6.1 Evaluation of Pitting Corrosion

Mitrovic-Scepanovic and Brigham[48] found that the critical concentration of chloride that causes pit initiation on a number of Mg alloys falls in the range of 2×10^{-3} to 2×10^{-2} *M* NaCl. The appearance, morphology, distribution, and depth of pits (i.e., the average penetration of the 10 deepest pits and the deepest one) should be determined in parallel with pitting potential determinations.[1,8] The statistical distribution of pits and the morphology of the pit should be examined by different microscopic technologies. The susceptibility of Mg alloys to localized corrosion can be evaluated as that of an alloy having an active-passive behavior in certain media by cyclic voltammetric, potentiodynamic, galvanostatic, scratch potentiostatic, and triboellipsometric methods, pit-propagation rate curves, impedance spectroscopic studies, and electrochemical noise measurements. Time-to-perforation data can be obtained by designing a specimen that is pressurized with air. This pressure

is monitored over a period of time until failure is indicated by a decrease in pressure.[1,48]

ASTM standard F 746-87 (i.e., "Pitting or Crevice Corrosion of Metallic Surgical Implant Materials") is designed to determine comparative laboratory indices of performance and can be used to rank materials in the order of increasing resistance to pitting and crevice corrosion. The test method given in ASTM standard F 746-87 covers the determination of the resistance to either pitting or the crevice corrosion of passive metals and alloys from which surgical implants will be produced. The resistance of surgical implants to localized corrosion is carried out in dilute sodium chloride solution (9 g/L) under the specific conditions of the potentiodynamic test method. Typical transient decaying curves under potentiostatic polarization should be interesting and are recommended for implants made of Mg alloys.

The E_{corr} of the working electrode (specimen) is recorded for 1 h in the NaCl solution (E_1). The current is recorded at +0.8 V/SCE for a period of time that depends upon the reaction. If localized corrosion is not stimulated in the initial 20 s, the polarizing currents will remain very small or will decrease rapidly with time. The stimulation of localized corrosion is marked by increasing polarization current with time or by current densities that exceed 500 $\mu A/cm^2$. The test consists of alternating between stimulation at 0.8 V/SCE and returning to a preselected potential (i.e., E_1 + a jump of +50 mV) until continuous increases or large fluctuations in current occur during the 15 min observation period. Evidence of pitting and crevice corrosion should be noted. This procedure is strongly recommended for Mg alloys that are in development for use in human body implants.[49]

6.2 Evolution of E_{corr} and Pitting

In a 0.1 *M* NaCl air-saturated solution without peroxide additions, the free E_{corr} of Mg and some of its alloys was measured to be in the range of −1500 to −1600 mV versus SCE for chloride concentrations of 5×10^3 to 5×10^4 M. In these solutions, no visible localized attack occurred, but a weight loss of approximately 5 mdd (which is equivalent to a current density of 5 $\mu A/cm^2$) was measured. On the other hand, with the addition of peroxide, the potential becomes much more noble, and the effect of the critical chloride concentration becomes clear. With 0.005 *M* NaCl, localized corrosion occurs, and the potential remains below the H line (approximmately −1.009 mV versus SCE at pH 13), which is indicative of a corrosion mechanism in which H reduction is the cathodic reaction. With 0.0005 *M* NaCl, no localized attack occurs, and the potential shifts toward very noble values. Localized attack is observed only when the free E_{corr} adopts a value active to the H line (Fig. 4).[48]

For aluminum, the suggested solution is 1 *M* sodium chloride and 9 ± 1 mL 30% hydrogen peroxide per liter at 25 °C. The period of immersion is on the order of 1 h, and the average value for the last 30 min should be within ±5 and ±10 mV for duplicate specimens.[8]

An increase in the chloride level to the critical value for each alloy, leading to the onset of localized corrosion, is accompanied by a shift in free E_{corr} to a value active to the hydrogen line, thereby making the production of hydrogen

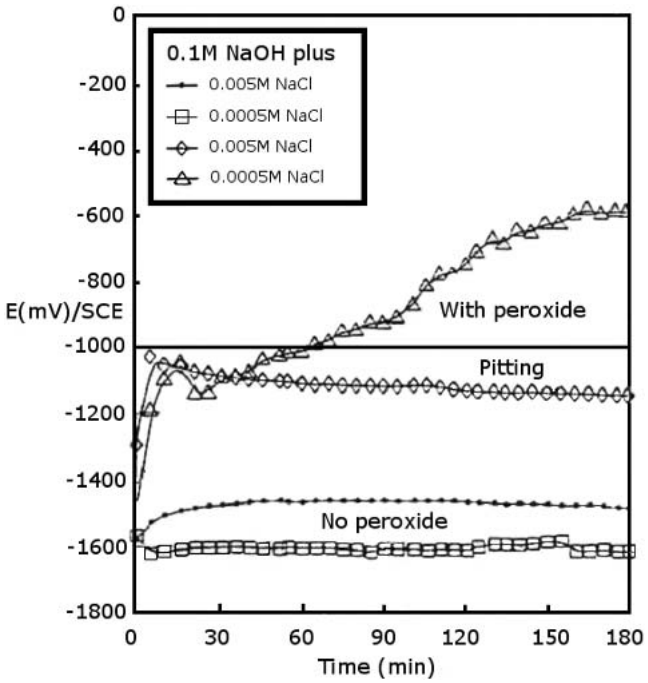

Fig. 4 E_{corr} of Mg in a 0.1 *N* NaOH solution. The H evolution reaction was around −1.009 V/SCE at pH 13 (Mitrovic-Scepanovic and Brigham[48]).

thermodynamically possible. This proposes that hydrogen is a prerequisite for localized corrosion.[1,48]

It is possible to use the pH change with time as a measure of the pitting corrosion resistance of Mg alloys. In acidic solutions, pitting is initiated mainly by the reduction of hydrogen ions, but in neutral solutions, the reduction of dissolved oxygen plays a major role during pitting. At a relatively high E_{corr} at the initiation step, oxygen consumes H ions. In neutral or weakly acidic solutions, two steps of pitting were clear: initiation and propagation. Between these two steps, there is a retention period that can vary in length according to the corrosion resistance of the alloy and that disappears completely at pH 1.25 in a 5% aerated sodium chloride solution.[42,50]

In many Mg alloys, the E_{oc} is higher than the pitting potential, and, thus, the pitting potential cannot be determined with the traditional methods. However, when the solution is mild and the alloy shows a good active-passive behavior, cyclic voltammetry can be used. The polarization curve showing the active-passive behavior for a Mg alloy (with or without a coating), and as a function of increasing chloride concentration, E_{bd} and E_{prot} can be determined. The breakdown potential (E_{bd}) corresponding to the considerable increase of the anodic current at a certain scan rate gives the susceptible condition for the initiation of localized attack. The more noble the breakdown potential, the more resistant the alloy will be to pitting and crevice corrosion. The potential at which the loop is completed upon reverse polarization determines the potential below which there is no localized attack (E_{prot}) for this scan rate. The obtained values are dependent on the scan rate. Also, allowing too much pitting propagation to occur along with the accompanying chemistry changes can influence the reversal in the scan rate.[1,8,50,51]

The quality of the passivation depends on the solution parameters, pH, chloride concentration if any, agitation, and temperature. For example, in ASTM standard D 1384 corrosive water saturated with $Mg(OH)_2$ at pH 10.6 and 25 °C, the critical passivation current and the passivation current are higher than 100 $\mu A/cm^2$ for pure Mg and lower than 10 $\mu A/cm^2$ for AZ91D alloy (die cast). It is not only the absolute value of the passivation potential that counts for an easy passivation, but also the difference between the passivation potential and the E_{corr}; this indicates the potential polarization required to attain passivation.[31] The good corrosion resistance of the thixomolded AZ91D alloy was electrochemically verified in a 0.17 mol/L NaCl solution saturated with $Mg(OH)_2$ by the presence of an important pseudo-passivation in NaCl solution with a small $i_{passive}$ and a noble E_{bd}.[16,51-53]

For a NaCl solution of 3.56 wt.% that has been deaerated at 25 °C, it is believed that concentrations up to 0.05-0.1 *M* should be sufficient to identify the relative resistance of Mg alloys in an alkaline solution of magnesium or sodium hydroxides at about pH 11-13.[21] The scan rate should be around 0.1-0.2 mV/s, instead or much less than 6 mV/s for iron-, nickel-, or cobalt-based alloys.[49]

Scan rates from 0.05-0.2 mV/s may give the standard active-passive behavior, otherwise scan rate of 0.01-0.04 mV/s can be tried and argon or nitrogen should be bubbled to remove oxygen from the solution.[8] Passive films can be formed by potentiostatic polarization for 10-15 h at a relatively noble potential, which is just enough for passivation to occur. The breakdown of the films can be determined by holding the sample in the electrolyte at a potential higher than E_{bd} until localized corrosion occurs. Another possibility is to initiate pits above the pitting or breakdown potential and then shift to lower values above or below the protection potential. It is assumed that at imposed values below the protection potential, one should observe a current decrease until complete repassivation occurs. At constant chosen currents, the evolution of potential as a function of time is recorded until the time rate of change in potential approaches zero. This technique is under development for aluminum alloys.[8]

In the so-called scratch-repassivation method for localized corrosion, the alloy surface is scratched and exposed to a constant potential. The current change is monitored as a function of time, and this will show the influence of potential on the induction time and the repassivation time. A careful choice of the level of potential between the breakdown potential and the critical pitting potential can give the critical pitting potential for a certain material in certain environmental conditions.[1]

6.3 Crevice Corrosion

The methods of analysis described in ASTM standard G 78-01 provide a guide for crevice corrosion testing of iron- and nickel-based alloys in seawater, especially with respect to the importance of the crevice geometry and specimen preparation on the obtained results.[1,8]

The crevice assembly described could be installed on any alloy type in any environment if crevices are being studied.[1] The Materials Technology Institute (MTI) of the Chemical Process Industry has identified five corrosion tests for iron- and nickel-based alloys, of which MTI-4 could be the most appropriate for Mg alloys. The MTI-4 method uses an increase in neutral bulk Cl^- concentration at eight levels, ranging from 0.1-3% NaCl, to establish the minimum critical Cl^- concentration that produces crevice corrosion at RT (20-24 °C).[54]

6.4 Filiform Corrosion

It has been mentioned that filiform corrosion was commonly observed and tended to occur at lower chloride concentrations than pitting. The critical chloride concentration for the initiation of localized corrosion (filiform and pits) was less than 0.05 *M* for several of the alloys tested. Weight loss increased with increased chloride concentration. Increases in temperature from 25-50 °C showed a minor effect in promoting the initiation of localized corrosion. Mg without intentional alloying additions showed exfoliation in which individual grains were preferentially attacked along crystallographic planes.[21]

6.5 Intergranular Corrosion

An innovative procedure should be considered for this purpose since there is no special targeted ASTM standard procedure for the intergranular corrosion of Mg. Susceptibility to this type of attack depends primarily on the type of alloy, the fabrication process, and the presence of efficient cathodic sites at the interface. The standard practice ASTM standard G 110-92 that evaluates the intergranular corrosion resistance of heat-treatable aluminum alloys by immersion in sodium chloride and hydrogen peroxide solution could be the most adaptable standard for testing intergranular attack in Mg alloys.[8] According to this standard, an immersion period of 6 h in a solution containing 57 g sodium chloride and 10 mL/L hydrogen peroxide (30%) is recommended. A metallographic cross section that is approximately 20 mm in length, preferably through a corroded area, should be examined. The type, extent, and depth of intergranular corrosion can be determined.[2,8] It is very possible that a less concentrated sodium chloride test solution could be appropriate for testing Mg alloys. For simple etching, for surface cleaning, and for microscopic observation or testing purposes, an immersion for 1 min into a boiling 20% CrO_3 solution with 1% silver nitrate is usually sufficient.

6.6 Galvanic Corrosion

Galvanic corrosion can give uniform and/or localized corrosion information. For example, pitting is observed in 5% sodium chloride solutions at an acidic pH of 1.25. However, well-defined pitting corrosion is common in neutral and alkaline solutions. Corrosion testing for galvanic corrosion can be predicted specifically by ASTM standards in the form of potential measurements. In general, the E_{corr} difference between the anode and cathode becomes the driving force for galvanic corrosion. A galvanic corrosion test between low-carbon steel and Mg alloys (NA42/AZ91D) was performed in an acid-chloride solution (pH 5.4, 200 ppm Cl^-) at the ambient laboratory temperature (22 ± 2 °C) to compare the galvanic effect. The galvanic currents were measured using a zero resistance ammeter (ZRA) for 7 h. The ratio of the anode area to the cathode area of the specimen was 1:1. Although the Mg-4Ni-*x*Al alloys had lower corrosion resistance than AZ91D, the

results of comparative galvanic corrosion tests between the low-carbon steel and the Mg alloys indicated that the galvanic corrosion resistance was higher in the Mg-4Ni-2Al (NA42) alloy than in AZ91D alloy.[43]

7. Impedance Measurements

Impedance measurements are usually performed at the E_{oc} and under potentiostatic conditions. Impedance measurements are appropriate to show the influence of mechanical deformation on surface electrochemical reactions.[29] Impedance measurements are carried out in a tetraborate buffer solution (0.05 *M* at pH 9.7). The scanned frequency ranged from 6 mHz to 100 kHz. The Nyquist plots of both Mg alloys at open circuit exhibit two capacitive loops, one for high and intermediate frequencies and the other, the small one, for low frequencies. The first capacitive loop is attributed to the charge-transfer process. Thus, for frequencies higher than 1 Hz, a resistor R_p and a capacitor double-layer capacitance (C_{d1}) in parallel can model the electrode/electrolyte interface. A partial data fitting made with the Boukamp circuit equivalent software for the charge-transfer process produced the R_p and C_{d1} values.[55]

The R_p values for the charge-transfer process were 207.7 and 374.0 Ωcm^2, respectively, for the AM50 and AZ91D alloys. The obtained capacitance values were 22.6 and 68.0 $\mu F/cm^2$, respectively, for the AM50 and AZ91D alloys. The slightly lower value of C_{d1} for the AM50 alloy implies the formation of a thick, protective film on the electrode surface, with the much lower C_{d1} values having already been reported for other Mg-based alloys.[56] The second small capacitive loop is generally attributed to mass transfer in the solid phase, which consists of the oxide/hydroxide layers.[57]

Over an immersion period of 72 h for the die-cast AZ91D alloy in ASTM corrosive water saturated with magnesium hydroxide (pH 10.6), the transfer resistance (R_t) increased gradually due to the formation of a protective corrosion film. A discontinuity during the first 10 h was linked to a partial degradation of the coating, a process that is irreversible. This behavior is closely related to the microstructure and composition of this alloy.[31] Maximum R_t values were on the order of 17 $k\Omega cm^2$ but dropped to about 5 $k\Omega cm^2$ during the 72 h immersion. Mathieu et al.[31] reported that the potential amplitude is set normally to 5 mV, and the frequency range is set between 10 kHz and 5 MHz. Generally, high and low capacitive loops are seen. The high-frequency capacitive loop can be attributed to charge-transfer reactions, and the diameter of the loop can be attributed to the R_t. The capacitance values for this loop were always below 50 $\mu F/cm^2$ and can be attributed to the C_{dl} of the partially covered surface. C_{dl} values were on the order of 5-10 $\mu F/cm^2$ and increased progressively to about 20 $\mu F/cm^2$. The second capacitive loop is generally attributed to the diffusion of ions through the hydroxide or oxide coating. Generally, the C_{dl} should decrease with the increase of passivity, and it was observed that the evolution of the C_{dl} was not in agreement with the covering of the surface as a function of the 72 h immersion of the die-cast AZ91D alloy in ASTM standard D 1384 corrosive water saturated with magnesium hydroxide. It can then be stated that the high-frequency loop can be related to the charge transfer and the surface film formation, as in the case of pure Mg.[8,37,58]

The electrochemical impedance spectra (EIS) spectra obtained under anodic polarization inside the potential range of MgO formation exhibit one capacitive loop followed by a linear part for both Mg alloys. An increase in R_p, which is significant in the case of the AZ91D alloy, suggests that the layer is growing on the electrode surface. The equivalent circuit consists of a resistor (R_p) in series with a constant-phase element (CPE), the two being connected with a capacitor (C_{d1}) in parallel. The CPE can be assumed to be Warburg diffusion according to the *n* values close to 0.5. Thus, under anodic polarization, the corrosion process is controlled by the mass transfer of the corrosion products through the oxide layers. The Nyquist plots for both Mg alloys obtained under cathodic polarization present one loop that is capacitive, which was attributed to the water reduction.[29,59]

8. Electrochemical Noise Technologies

New and accurate technologies are required to investigate the rather fast kinetics of localized corrosion. Electrochemical noise is an interesting tool that is used to monitor metastable pitting, which operates by recording the galvanic current between nominally identical electrodes on the E_{corr} of a single electrode. The spatial separation of the anodic processes in the pit and the cathodic processes on the surrounding surfaces necessitates the passage of current that gives rise to the measured noise signals.[60]

Since localized corrosion sites are typically very small, on the order of 100 μm in diameter or less, the current densities inside these cavities can be on the order of 1 A/cm^2, which can be detected. Electrochemical noise studies can be performed under E_{oc}, very close to the natural conditions of pitting. However, to complete the electrochemical studies and distinguish between repassivating superficial pits and penetrating ones, microscopic studies are highly desirable. The scanning reference electrode technique (SRET) should be an excellent complementary tool.[60]

The corrosion behavior of the Mg alloy AM60 has been investigated by electrochemical noise measurements made in chloride and sulfate solutions. Galvanostatic tests in combination with the measurements of the current noise were useful in determining the breakthrough potential in a 0.01 *M* aerated sodium sulfate solution. In this study, the potential was stabilized for 30 min in the open circuit and then was subjected step by step to a gradually increasing imposed current (galvanostatic mode). The potential-time noise diagram showed oscillations that were characteristic of the pitting phenomena at a certain level. The potentials determined from this method were found to be very similar to those obtained by cyclic voltammetry for the same conditions using a scan rate of 0.1 mV/s for a current density of 1 mA/cm^2. This technology helped to examine the influence of different corrosion inhibitors.[33]

Noise measurements were carried out for two Mg alloys, AZ91D and ZA1040, in a 5% sodium chloride solution saturated with magnesium hydroxide. The sample was not subjected to an external applied current. The corrosion rate can be obtained from an estimate of the polarization resistance, R_p,

which is inversely related to the linear corrosion rate by the Stern-Geary approximation. Three approaches are possible for obtaining R_p from the electrochemical noise (EN) current and potential measurements: noise resistance, spectral noise resistance, and self-linear polarization resistance. The latter is used in this work because it seems to be more accurate than the other two. The corrosion rate was found to be much higher for the experimental alloy than for the AZ91D alloy. The results were supported by scanning electronic microscopy and in situ measurements using the SRET.[53]

Zhang et al.[61] studied the aluminum alloy LY12 in a 1 *N* sodium chloride solution with electrochemical noise and impedance techniques. They found that the fractal dimension (D_n) obtained from spectral power density (SPD) was mainly directly proportional to the intensity of pitting corrosion or the value of the pitting parameter (S_E) derived from dimensional analysis, while the fractal dimension (D_E) obtained from EIS was mainly related to the uniform corrosion.

9. The SRET

The SRET has enabled the measurement of localized current densities in the vicinity of pits in a stainless steel in natural water. Novel applied potentiodynamic pitting scans have been obtained for localized areas immediately adjacent to accurately defined regions of the electrode surface.[62]

Isaacs has made a good design of the SRET to study the pitting and intergranular corrosion in stainless steels. He is also associated with the scanning vibrating electrode technique (SVET), in which the probe is mounted on a biomorph piezoelectric reed that vibrates the tip normal to the electrode at a characteristic frequency.[63] Another variation of the technique has been used in the localized measurement of electrochemical impedance spectra (LEIS).[64]

The commercially fabricated SRET consists of a pair of platinum electrodes made of a wire that is 0.2 mm in diameter. The probes have electrochemically sharpened tips of an approximate radius of 1 μm and, apart from the tips, have as little platinum exposed to the electrolyte as possible. One tip is close to the metal surface and samples the electric field created by the ion flux (10-20 μm from the metal). The other probe, placed a few millimeters behind the first, samples the noise in the bulk electrolyte. The output from the platinum electrodes is taken to an alternating current (ac)-coupled differential amplifier before being digitized into a form that the computer can use and display.[62] The description of the electrochemistry of the method has been provided by Eden.[65]

Quantifying the degree of localized corrosion in terms of current density, as opposed to simply measuring the amplitude of the electric field adjacent to the source of activity, is a challenging goal in the use of SRET. The point in space (SPI) is a reference calibration signal for a known current that has been derived from an electrode of known surface area. Every specific metal/interface with operational conditions should have certain characteristics for better, more sensitive signals, and Mg has its special characteristics with a passive nonperfect covering layer.

SRET measurements were carried out for two Mg alloys, AZ91D and ZA1040, in a solution of 5% sodium chloride saturated with magnesium hydroxide. In this approach, the micropotential gradients in solution just above the surface of the material under study are recorded. The micropotential gradient in the solution that is perpendicular to the surface is proportional to the ionic current either leaving from or going toward the surface. The potential difference is equal to the ionic current times the solution resistance. The SRET maps of potential difference, or equivalently ionic current, over both samples are shown at two different times (i.e., 20 min and 8 h). The SRET studies illustrated that localized corrosion occurred more frequently on the ZA1040 sample than on the AZ91D sample. The location of localized corrosion was also much more likely to change on the ZA1040 sample than on the AZ91D sample.[52]

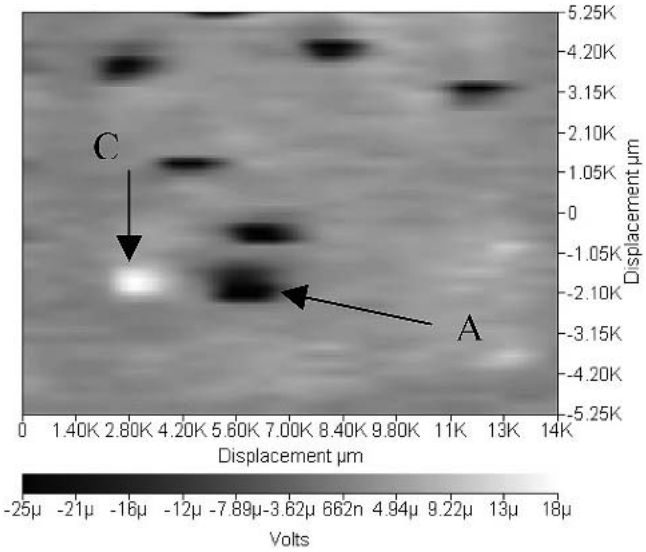

Fig. 5 Two-dimensional SRET map of a ZACS 1040305 alloy after 48 min in a solution of 5% NaCl saturated with magnesium hydroxide. C, cathode; A, anode[52]

Figure 5 gives a two-dimensional SRET map of a ZACS1040305 alloy and shows the distribution of pits on the surface after only 48 min in a solution of 5% NaCl that was saturated with magnesium hydroxide. As a function of time, some of the pits were blocked, giving rise to pits growing in other sites. This behavior was closely related to the microstructure and the alloying elements since the commercial AZ91D showed a different pattern.

The SVET that has been used to examine the performance of coatings is composed of the microelectrode, scanning system, measurement system, and so on. The distance from the surface of the specimen to the microelectrode was held at a constant distance of 8 μm. The oscillation frequency was 625 Hz, the amplitude of vibration of the microelectrode was 0.5 μm, and the scanning range was 1.5 mm^2. Thermal spray coatings of WC-CO were studied. The distribution of potential on the surface of the coating (8 μm distance between the electrode and the surface of the specimen) was measured using the SVET. However, because the pores were very small, information on the locations of the distributed potential could not be obtained. Using a Vickers hardness tester, indentations were made on the coating (i.e., a 50 g load with a diagonal length equal to 405 μm) to induce an artificial defect, and,

considering a pore model short-circuited between the base and the solution, temporal changes in the potential distribution on the coating surface (8 μm distance) were investigated. Such studies can be extrapolated to examine passive Mg alloys. Of course, such corrosion behavior varies with changes in chemical and coating characteristics.[66]

Acknowledgments

Thanks are given to Dr. Norbert Hort from GKSS for fruitful discussions and M. Pierre Gelinasing, Jr. B.Sc. in metallurgical engineering for revision and help.

References

1. *Corrosion,* Vol 13, 9th ed., *Metals Handbook,* ASM International, 1987, p 193-196, 207-220, 231-233, 303-310
2. B.W. Lifka, Aluminum (and Alloys), *Corrosion Testing and Standards: Application and Interpretation,* R. Baboian, Ed., American Society for Testing and Materials, 1995, p 447-457
3. NACE: Metals Section, *Corrosion Data Survey,* 6th ed., NACE International, The Corrosion Society, 1985
4. *Handbook of Corrosion Data,* B.D. Craig and D.S. Anderson, Ed., ASM International, 1995
5. D.J. De Renzo, *Corrosion Resistant Materials Handbook,* 4th ed., D.J. De Renzo, Ed., Noyes Data Corporation, 1985
6. P.A. Schweitzer, *Corrosion Resistance Tables: Metals, Plastics, Nonmetallic and Rubbers,* 2nd ed., Marcel Dekker, 1986
7. G.L. Song, A. Atrens, and M. Dargusch, Influence of Microstructure on the Corrosion of Diecast AZ91D, *Corrosion Sci.* Vol 41, 1999, p 249-273
8. GI 6-95 Standard Recommended Practice for Applying Statistics to Analysis of Corrosion Data, *Annual Book of ASTM Standards,* Vol 03-02, p 69-82
9. W.K. Miller and E.F. Ryntz Jr., "Magnesium for Automotive Applications: A State-of-the-Art Assessment, Localized Corrosion," paper 83-0521, Society of Automotive Engineers, 1984
10. A. Stalmann, W. Sebastian, H. Friedrich, S. Schumann, and K. Droder, Properties and Processing of Magnesium Wrought Products for Automotive Applications, Adv. Eng. Mater., Vol 3 (No. 12), 2001, p 969-976
11. E. Aghion and B. Bronfin, Global Overview on Demand and Applications for Magnesium Alloys, Magnesium Alloys Development Towards the 21st Century, *Mater. Sci. Forum,* Vol 350-351, 2000, p 19-28
12. E. Aghion, B. Bronfin, F. Von Buch, S. Schumann, and H. Friedrich, Dead Sea Magnesium Alloys Newly Developed for High Temperature Applications, *Magnesium Technology,* H.I. Kaplan, Ed., The Minerals, Metals & Materials Society, 2003, p 177-182
13. R.L. Edgar, Global Overview on Demand and Applications for Magnesium Alloys, *International Congress Magnesium Alloys and Their Applications,* K.U. Kainer, Ed., 26-28 Sept 2000 (Munich), Wiley-VCH, 2000, p 3-8
14. A. Luo, M. Balogh, and B.R. Powell, "Tensile Creep and Microstructure of Magnesium-Aluminium-Calcium Based Alloys for Powertrain Applications: Part 2 of 2," paper 01-0423, Society of Automotive Engineers, 2001
15. H. Kaufman, R. Potzinger, and P.J. Uggowitzer, NRC, *Magnesium Castings for Structural Applications,* M. Sahoo and T.J. Lewis, Ed., Metallurgical Society of CIM (Montreal, Canada), Light Metals Métaux Légers, COM, 2001, p 216-223
16. I. Nakatsugawa, H. Takayasu, and K. Saito, Corrosion Behavior of Thin Wall Magnesium Products Molded by Thixomolding, *op. cit.* ref. 13, p 445-450
17. D.M. Walukas, R.F. Decker, R.E. Vining, and R.D. Carnahan, Thixomolding of Magnesium, *Magnesium 97 Proceedings of the First Israeli International Conference on Magnesium Science & Technology,* E. Aghion and D. Eliezer, Ed., 10-12 Nov 1997 (Dead Sea), p 54-59
18. C. Jaschik, H. Haferkamp, and M. Niemeyer, New Magnesium Wrought Alloys, *op. cit.* ref. 13, p 41-46
19. W. Sebastian, K. Dröder, and S. Schumann, Properties and Processing of Magnesium Wrought Products for Automotive Applications, *op. cit.* ref. 13, p 602-608
20. G.L. Song and A. Atrens, Corrosion Mechanisms of Magnesium Alloys, *Adv. Eng. Mater.,* Vol 1 (No. 1), 1999, p 11-33
21. R.J. Brigham, "Localized Corrosion Initiation on Magnesium Alloys," Report No. MTL 90-51(TR), CANMET, 1990
22. M.M. Avedesian and H. Baker, Ed., *ASM Specialty Handbook: Magnesium and Magnesium Alloys,* ASM International, 1999, p 138-162, 194-215
23. J.D. Hanawalt, C.E. Nelson, and J.A. Peloubet, Corrosion Studies of Magnesium and Its Alloys, *Trans. Am. Soc. Mining Metall. Eng.,* Vol 147, 1942, p 273-299
24. G. Song, A. Atrens, D. St. John, J. Nairn, and Y. Li, The Electrochemical Corrosion of Pure Magnesium in 1 N NaCl, *Corrosion Sci.,* Vol 39 (No. 5), 1997, p 855-875
25. G. Song, A. Atrens, D. St John, X. Wu, and J. Nairn, The Anodic Dissolution of Magnesium in Chloride and Sulfate Solutions, *Corrosion Sci.,* Vol 39 (No. 10-11), 1997, p 1981-2004
26. G. Song and A. Atrens, Corrosion Behaviour of Skin Layer and Interior of Die Cast AZ91D, *Proceedings, Fourth International Conference on Magnesium Alloys and Their Applications,* B.L. Mordike and K.U. Kainer, Ed., 28-30 April 1998 (Wolfsburg, Germany), Wekstoff-Informationsgesellschaft GmbH, 1998, p 415-419
27. P.P. Trzaskoma, Corrosion Behavior of a Graphite Fiber/Magnesium Metal Matrix Composite in Aqueous Chloride Solution, *Corrosion,* Vol 42 (No. 10), 1986, p 609-613
28. E.M. Gutman, A. Eliezer, Ya. Unigovski, and E. Abramov, Mechan-electrochemical Behavior and Creep Corrosion of Magnesium Alloys, *Mater. Sci. Eng.,* Vol 302, 2001, p 63-67
29. P.L. Bonora, M. Andrei, A. Eliezer, and E.M. Gutman, Corrosion Behaviour of Stressed Magnesium Alloys, *Corrosion Sci.,* Vol 44, 2002, p 729-749
30. H. Inoue, K. Sugahara, A. Yamamoto, and H. Tsubakino, Corrosion Rate of Magnesium and Its Alloys in Buffered Chloride Solutions, *Corrosion Sci.,* Vol 44, 2002, p 603-610
31. S. Mathieu, C. Rapin, J. Hazan, and P. Steinmetz, Corrosion Behavior of High Pressure Die-Cast and Semi-Solid Cast AZ91D Alloys, *Corrosion Sci.,* Vol 44, 2002, p 2737-2756
32. P. Adeva-Ramos, S.B. Dodd, P. Morgan, F. Hehmann, P. Steinmetz, and F. Sommer, Autopassive Wrought Magnesium Alloys, *Adv. Eng. Mater.,* Vol 3 (No. 3), 2001, p 147-152
33. R. Feser and J.W. Erning, Electrochemical Noise Measurements for the Determination of the Effectiveness of New Corrosion Protection Layers on Aluminum and Magnesium, *Mater. Corrosion,* Vol 52, 2001, p 456-461
34. E.D. Morales, E. Ghali, N. Hort, W. Dietzel, and K.U. Kainer, Corrosion Behavior of Magnesium Alloys with RE Additions in Sodium Chloride Solutions, Magnesium Alloys 2003 Part 1, *Proceedings of the 2nd International Conference on Platform Science and Technology for Advanced Magnesium Alloys,* Y. Koshima, T. Aizawa, K. Higashi, and S. Kamado, Ed., 26-30 Jan 2003 (Osaka, Japan), Trans Tech Publications Ltd, 2003, p 867-872
35. O. Lunder, T.K. Aune, and K. Nisancioglu, Effect of Mn Additions on the Corrosion Behavior of Mould-Cast Magnesium ASTM AZ91, *Corrosion,* Vol 43, 1987, p 291-295
36. T. Beldjoudi, C. Fiaud, and L. Robbiola, Influence of Homogenization and Artificial Aging Heat Treatments on Corrosion Behavior of Mg-Al Alloys, *Corrosion,* Vol 49, 1993, p 738-745
37. G. Baril and N. Pebere, The Corrosion Behavior of Pure Magnesium in Aerated and Deaerated Sodium Sulfate Solution, *Corrosion Sci.,* Vol 43, 2001, p 471-484
38. G. Song, A. Atrens, and D. St. John, An Hydrogen Evolution Method for the Estimation of the Corrosion Rate of Magnesium Alloys, *Magnesium Technology*, J. Hryn, Ed., The Minerals, Metals & Materials Society, 2001, p 255-262
39. B.L. Tiwari and J.J. Bommarito, A Novel Technique to Evaluate the Corrosion Behavior of Magnesium Alloys, *Magnesium Technology,* H.I. Kaplan, Ed., The Minerals, Metals & Materials Society, 2002, p 269-275
40. A.F. Froats, T.K. Aune, D. Hawke, W. Unsworth, and J. Hillis, *Corrosion,* Vol 13, 9th ed., *Metals Handbook,* ASM International, 1987, p 740-754

41. J.I. Skar and D. Albright, Corrosion Behavior of Die-Cast Magnesium in ASTM B117 Salt Spray and GM9540P Cyclic Corrosion Test, *op. cit.* ref. 12, p 59-63
42. D. Weiss, B. Bronfin, G. Golub, and E. Aghion, Corrosion Resistance Evaluation of Magnesium and Magnesium Alloys by an Ion Selective Electrode, *Magnesium 97, Proceedings of the First Israeli International Conference on Magnesium Science & Technology,* E. Aghion and D. Eliezer, Ed., 10-12 Nov 1997 (Dead Sea), 1997, p 208-213
43. Y.-S. Choi, J.-G. Kim, S.K. Kim, and Y.-J. Kim, Aqueous Corrosion Characteristics of Mg-4Ni-xAl Alloys in Acid-Chloride Solution, *op. cit.* ref. 39, p 277-282
44. P. Roberge, Acceleration and Amplification of Corrosion Damage, *Handbook of Corrosion Engineering,* McGraw Hill, 1999, p 486-576
45. O. Lunder, J.E. Lein, S.M. Hesjevik, T.K. Aune, and K. Nisancioglu, Corrosion Morphologies on Magnesium Alloy AZ91, *Werkstoffe Korrosion,* Vol 45, 1994, p 331-340
46. L. Ciaghi, L. Fedrizzi, F. Deflorian, and P.L. Bonora, Evaluation of the Corrosion Rate of Mg/Al Zn Alloys, *International Congress Magnesium Alloys and Their Applications* (Garmich, Germany), Wiley-VCH, 1992, p 151-158
47. C.F. Baker, New Alloys and Shot Delivery System Developments, *Magnesium Alloys and Their Applications,* B.L. Mordike and F. Hehman, Ed., Informations Gesellschaft, 1992, p 77-87
48. V. Mitrovic-Scepanovic and R.J. Brigham, Localized Corrosion Initiation on Magnesium Alloys, *Corrosion,* Vol 48 (No. 9), 1992, p 780-784
49. "Standard Method for Pitting of Crevice of Metallic Surgical Implant Materials," F 746-87, *1997 Annual Book of ASTM Standards,* ASTM, Vol 13.01, p 181-186
50. B.-Y. Hur and K.-W. Kim, A New Method for Evaluation of Pitting Corrosion Resistance for Magnesium Alloys, *Corrosion Rev.,* Vol 16, 1998, p 85-94
51. I. Nakatsugawa, F. Yamada, H. Takaysu, T. Tsukeda, and K. Saito, Corrosion Behavior of Thixomolded Mg-Al Alloys, *Proceedings of the 38th Annual Conference METSOC, CIM, Environmental Degradation of Materials and Corrosion Control in Metals,* M. Elboujdaini and E. Ghali, Ed., 22-26 Aug 1999 (Quebec), p 113-123
52. M.O. Oteyaka, A.-M. Lafront, R. Tremblay, and E. Ghali, Pitting Corrosion of Some Magnesium Alloys by Scanning Reference Electrode Techniques (SRET), *NACE International Seminar Proceedings, Northern Area, Montreal Section, Session 2,* 26-27 Aug 2002 (Montreal)
53. A.-M. Lafront, M.O. Oteyaka, R.D. Klassen, P.R. Roberge, and E. Ghali, Study of the Corrosion of Zinc and Aluminium Magnesium Alloys by Electrochemical Noise (EN) and Scanning Reference Electrode Technique (SRET), *ibid.*
54. R.M. Kain, Crevice Corrosion Behavior of Stainless Steel in Sea Water and Related Environments, *Corrosion*, Vol 40 (No. 6), 1984, p 313-321
55. B.A. Boukamp, A Non Linear Least-Squares Fit Procedure for Analysis of Immittance Data of Electrochemical Systems, *Solid State Ionics,* Vol 20 (No. 1), 1986, p 31-44
56. R. Udhayan and D.P. Prokash Bhatt, *J. Power Sources*, Vol 63, 1996, p 103-107
57. S. Turgoose and R.A. Cottis, The Impedance Response of Film-Covered Metals, *Electrochemical Impedance: Analysis and Interpretation,* Scully, Silverman and Kendig, Ed., 1993, p 173-191
58. N. Pebere, C. Riera, and F. Dabosi, Investigation of Magnesium Corrosion in Aerated Sodium Sulfate Solution by Electrochemical Impedance Spectroscopy, *Electrochem. Acta,* Vol 35 (No. 2), 1990, p 555-561
59. C.H. Tsai, Analysis of EIS Data for Common Corrosion Processes, *op. cit.* ref. 57, p 37-52
60. R.G. Kelly, Pitting, *Corrosion Testing and Standards: Application and Interpretation,* R. Baboian, Ed., ASTM, 1995, p 166-174
61. J.Q. Zhang, Z. Zhang, J.M. Wang, H.B. Shao, and C.N. Cao, Corrosion Monitoring of LY12 in 1 N Sodium Chloride Solution with Electrochemical Noise Technique, *Acta Metall. Sinica,* Vol 14 (No. 2), 2001, p 91-96
62. K.R. Trethewey, D.A. Sargent, D.J. Marsh, and S. Haines, New Methods of Quantitative Analysis of Localized Corrosion Using Scanning Electrochemical Probes, Modelling Aqueous Corrosion From Individual Pits to System Management, NATO ASI Series, Series E: Applied Sciences, Vol 266, K.R. Trethewey and P.R. Roberge, Ed., 1994, p 417-442
63. L.F. Jaffe and R. Nuticelli, An Ultrasensitive Vibrating Probe for Measuring Steady Extracellular Currents, *J. Cell Biol.,* Vol 63, 1974, p 614-628
64. H.S. Isaacs and M.W. Kendig, Determination of Surface Inhomogeneities Using a Scan Probe Impedance Technique, *Corrosion,* Vol 36, 1980, p 269-274
65. D.A. Eden, Electrochemical Noise, *Uhlig's Corrosion Handbook,* W.R. Revie, Ed., John Wiley, 2000, Chap. 69, p 1227-1238
66. N. Morihiro, M. Takeda, G. Katayama, M. Kido, and Y. Harada, Corrosion Behaviour of WC Thermal Spray Materials, *Proceedings of the Second International Conference on Environment Sensitive Cracking and Corrosion Damage, "ESCCD,"* M. Matsumura, H. Nagano, K. Nakasa, and Y. Isomoto, Ed., 29 Oct-2 Nov 2001 (Hiroshima, Japan), Nishiki Printing Ltd, 2001, p 153-159